45TH TURBOMACHINERY & 32ND PUMP SYMPOSIA
HOUSTON, TEXAS | SEPTEMBER 12 – 15, 2016
GEORGE R. BROWN CONVENTION CENTER

Feasibility study on the use of side channel pumps for low viscosity fluids, with fracking or other hydrocarbon processing applications

Dipl.-Ing. Sebastian Fleder
Member of research staff
Technical University of Kaiserslautern
Insitiute for Fluid Mechanics and Fluidmachinery
Kaiserslautern, Germany

Dipl.-Ing. Frank Hassert
Head of R&D
SERO PumpSystems GmbH
Meckesheim, Germany

Prof. Dr.-Ing. Martin Böhle
Professor, Head of Faculty
Technical University of Kaiserslautern
Institute for Fluid Mechanics and Fluidmachinery
Kaiserslautern, Germany

Dipl.-Kffr. Beate Zientek-Strietz
CEO
SERO PumpSystems GmbH
Meckesheim, Germany

Sebastian Fleder
Academic studies at Technical University of Kaiserslautern, Mechanical Engineering, Diploma, Graduation 2011
Member of research staff at Faculty of Mechanical Engineering, Institute for Fluid Mechanics and Fluidmachinery since 2011
Field of Activity: Cavitation and mixed flow in Side Channel pumps, Journal Bearings for high loads, Windage Losses at large clearances for high speed rotating machinery, Compressors for Heat Pumps and Chillers

Frank Hassert
Academic studies at the University of Applied Sciences of Heilbronn, Germany, Precision Mechanics, Diploma, Graduation 1998
Design engineer – later chief designer - within the printing machine industry for nine years
Since 2007 Technical and Quality Manager with SERO PumpSystems GmbH in Meckesheim, Germany
Responsible for design and development of the complete range of side channel pumps (standard and customer solutions), supporting sales and service forces in technical matters and running operative QA / QC department

ABSTRACT

Side channel pumps typically are used in applications with low specific speed. The ratio of the low flow and high head tends to result in this niche product, located in between the classical displacement and centrifugal pumps, but uniting the advantages of both.
Best experience in the design of these multistage ring section pumps is in using bearing bushings in the stages that are lubricated by the pumping media itself. This guarantees them to be low in service and maintenance time and cost and the pump has no need for another lubricant which contaminates the pumped media. The side channel pumps are a good solution for use with low density (below 5.8 lb/gal / 700 kg/m³), and low viscosity hydrocarbons (lower than 4.3e-8 lbf s/in² / 0.3 cP), e.g. in fracking applications or petro-chemical use.
The investigated side channel pump is able to generate and handle high pressures at low flows, but in a number of hydrocarbon applications with low viscosities, low NPSH-values or with relatively high percentage of entrained gas, some material failure in the bearings is discovered.
The working principle of the pump and the performance characteristic is briefly explained. One of those characteristics is a highly transient pulsating pressure, resulting in high forces on the shaft and the impeller. The reasons for the pulsation and some methods to deal with the resulting forces are shown and explained.
The high radial load, together with the low viscosity, could lead to an overload of the standard bearings and material failure. New journal bearings have to be designed. Some other possible solutions and ways to deal with the high forces are shown.
The head and efficiency curves are tested on a test rig and the results are compared to numerical investigations. The pulsations and the force are determined in numerical investigations. The NPSH-value is measured and an optimized NPSH-impeller is designed and

manufactured using Rapid-Prototyping. The newly manufactured impeller is compared to the original design, manufactured in two different ways (sand casting and investment casting).
In the end, a modified pump, ready for the use in hydrocarbon-processing and fracking applications with amounts of gas and a low NPSH requirement is presented and the characteristics are tested on a test-rig, applying affinity laws.

OVERVIEW

In the first part of the paper, the pump type is briefly explained; the history and some of the main application are shown. Side channel pumps and their 'pump relatives' positive displacement and centrifugal pumps are classified and the working principle on water as well as the theoretical background for two-phase flow handling is briefly explained.
The following second part deals with the numerical approach and experimental investigations on a test pump. It shows the characteristic performance curve and NPSH3%-curve. These investigations show two subfields of improvements that are performed for the pump: bearings load capacity and NPSHR-value of the first stage impeller and whole pump.
Part three explains the need for bearing setup modification, based on observations of bearing failure of the pump. New bearings are designed, following the procedure explained in Appendix A. A test rig for journal bearings is shown and the experimental results are explained.
The forth part compares different NPSH impeller designs and their varying results also for different casting processes. It shows the new designed impeller as well as the characteristic curves for the generated head and NPSHR.
The last part finally summarizes the improvements on each of the subfields.

PART ONE: THEORETICAL BACKGROUND AND EDUCATIONAL CONTENT

History and main applications

Originally developed in Germany for water supply in private households prior to the full coverage of municipal water supply network, the side channel pump (SCP) was protected by patent in 1920. Characteristic for the side channel pump is the relatively high head at low flows. In addition this pump type is self priming and generally able to handle two-phase flow with a permanent content of up to 50% (by vol.) of gas, vapor or air in the process-fluid or up to 100% for a limited period of time. These properties determine the application range of the pump in the industry. Among others its main fields of operation are chemical engineering and processing, automotive, LPG distribution, food production, boiler feed, condensate recovery, etc.

Assembly and working principle

A single side channel pump stage is assembled as depicted in Figure 1. The impeller is mounted within two casing shells, one with a side channel on one side. The impeller consists of straight radial blades (2), which force the fluid in circumferential direction. It has no shrouds. The fluid leaves the impeller at the outer radius and enters the side channel. It is then transported to the inner radius of the impeller and re-enters it there. The fluid describes a spiral flow through the pump stage from the inlet (1) to the discharge port (3). Outlet and inlet are separated by the interrupter area or breaker. The process of leaving and re-entering the impeller several times is called inner multi stage effect. During this process, the pressure rises in radial and circumferential direction. However, a part of the fluid does not leave the pump through the discharge port at the end of the side channel (5), but fills the gap of the breaker area (4), is transported by the blades back to the suction end of the channel geometry and therefore sealing the discharge side from the suction side of the pump stage dynamically.

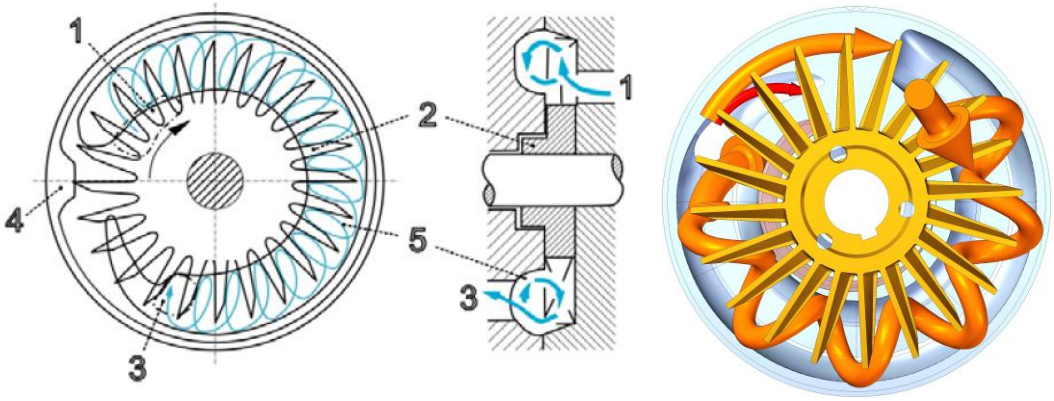

Figure 1: Assembly of a side channel pump and working principle (Fleder and Boehle, 2012)

When combining a SCP with an upstream radial impeller, very low NPSH3% values can be realized.
The SCP generates high pressure differentials between the several stages, which can be used to provide a lubrication film in the journal bearings. Due to this feature, the use of SCP in hygienic and dairy industry or other food processing applications is possible.
A lot of experimental studies examined the influences of the geometry on the characteristic curves for head and efficiency. The first approaches were made by Ritter (1930) and Schmiedchen (1932) who examined the influence of side channel and blade geometry on the performance of the pump. Later Surek (1998) analyzed the influence of the blade geometries in more detail.
Nowadays, due to the use of numerical methods it is possible to study the inner flow phenomena of the pump. By this way the influence of geometrical changes on the flow can be described and explained. The work of Böhle and Müller (2009) presents a method to combine the results of CFD with an analytical flow model. Fleder and Böhle (2012a) dealt with the inner flow phenomena of the pump as well as the blade shape of industrial side channel pumps (Fleder and Boehle, 2012b). The general simulation-process, the numerical setup and the post-processing in this effort are based on these investigations.

Two-phase Flow Handling

Side channel pumps are known to be a good choice when high amounts of gas are present in the liquid or when the pump needs to be self-priming.
Figure 2 shows the effect of different gas contents on the characteristic curve for classical radial centrifugal pumps and side channel pumps (unknown specific speed). For centrifugal pumps, an amount of 8% of gas has been detected as maximum gas volume fraction before these pumps stop working. Side channel pumps are able to handle larger amounts of gas with only small changes in the characteristics. The power consumption and efficiency decrease with rising gas volume for both pump types.
A combination of both impeller types as in the present pump with an NPSH-runner in front of several side channel stages hasn't been analyzed in detail, but it can be assumed that not the maximum gas amount of the centrifugal impeller is the limitation, as the side channel stage is working with a suction effect that simply evacuates the gas out of the NPSH-runner.

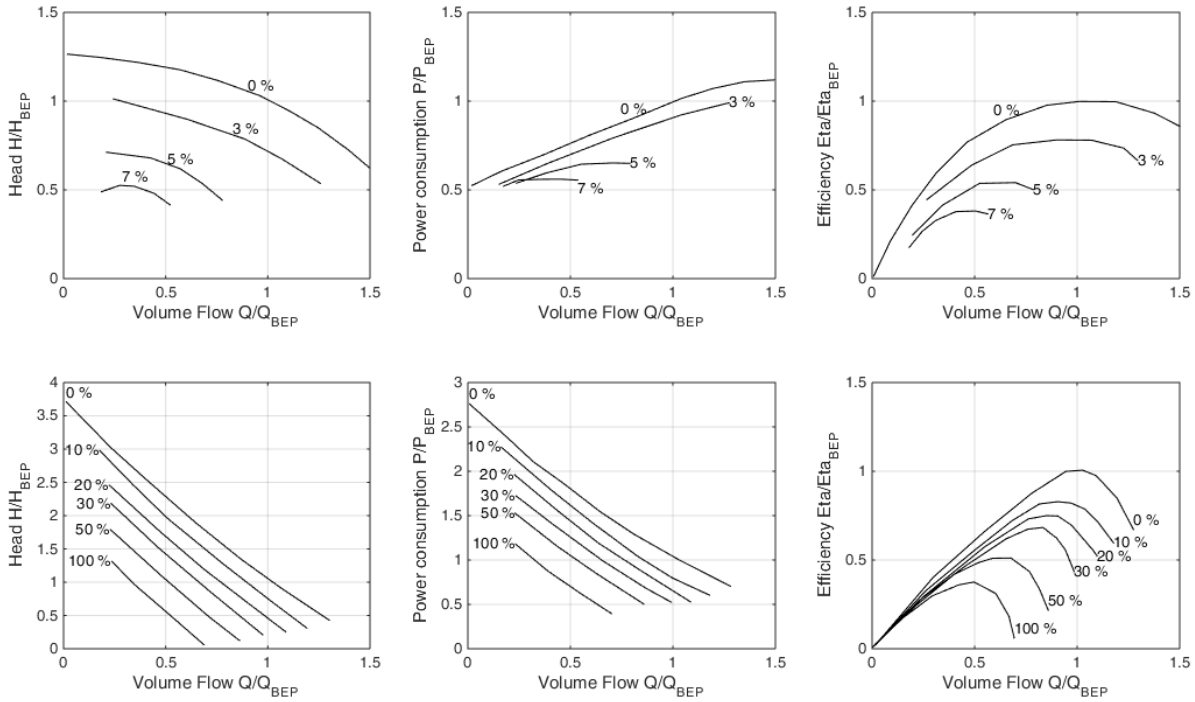

Figure 2: Effect of gas on performance of centrifugal pumps (top) and SCP (bottom) (Lehmann and Fandray, 1990)

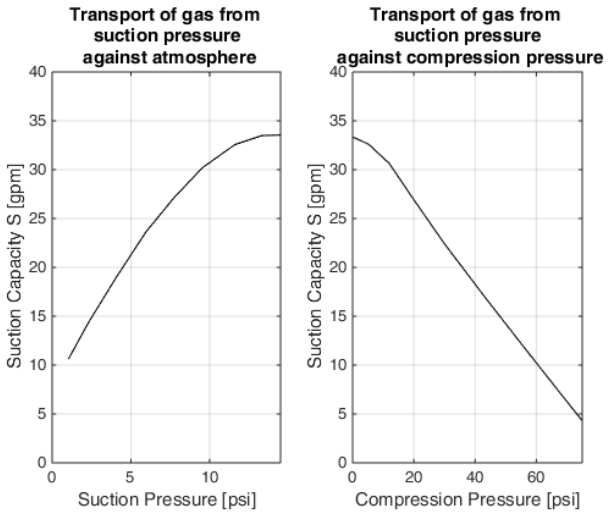

Figure 3: Suction capacity of SCP (Lehmann and Fandray, 1990)

At the beginning of the self-priming process, when the suction piping is empty, only gas/air is transported by the pump to the pressure piping. Meanwhile the fluid is primed automatically to the pump from the suction vessel. The speed, in which the air in the suction piping gets evacuated, depends on the pressure difference between suction and discharge side. Figure 3 shows an example for the suction speed capability of a classical side channel pump, investigated by Lehmann and Fandray (1990).

The theoretical considerations, formulated by Lehmann and Fandray (1990), Ritter (1930), and Surek (1998) explain the self-priming and two-phase-flow handling ability with the same working principle. The analogy to the working principle of water ring pumps assumes that due to centrifugal forces in the rotating impeller, a water ring is formed at the outer radius and the gas is mostly

transported near the shaft in the hub area. An additional gas outlet near the shaft in the interrupter area allows the gas to exit the pump stage. The schematic and an assembly for a pump with an gas outlet near the shaft is depicted in
Figure 4 and
Figure 5.
When gas-liquid mixtures are present in the suction piping, the theoretical consideration describes the flow state in the pump with the same working principle, the only difference now is the presence of liquid at the outlet port. The process of self priming works better at low rotational speeds and low differential pressures. The process of two-phase flow handling is discovered to be contrarily influenced. First tests show a better two-phase flow handling for the test pump at high rotational speeds and at low volume flows, which means higher differential pressures between inlet and outlet.

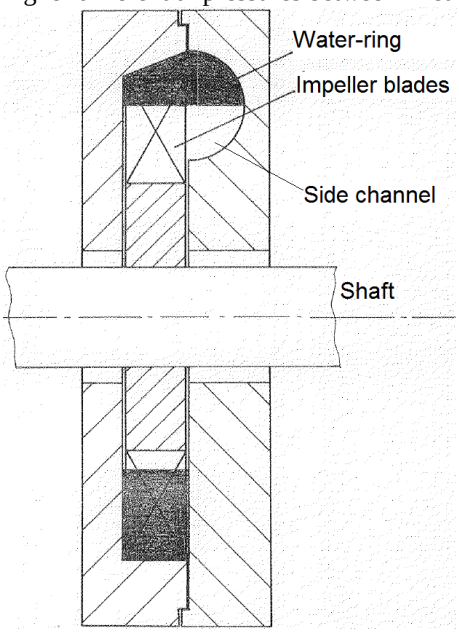

Figure 4: Flow state inside the SCP stage during self priming

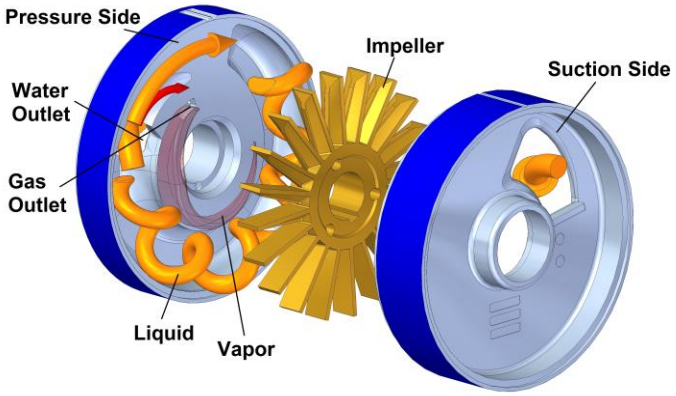

Figure 5: Working principle for self priming and two-phase flow handling

Classification of SCP

In the Cordier diagram, side channel pumps are located between positive displacement pumps and centrifugal pumps. The specific speed is low, which means high heads at low flows. On a first view, the maximum efficiency for those pumps seems lower than of classical centrifugal pumps which can reach 80% and higher. But at a closer look, centrifugal pumps at this specific speed work at the same efficiency as side channel pumps. The Cordier diagram and the maximum efficiency subject to the specific speed are shown in Figure 6 and Figure 7 where the specific speed n_q is defined as

$$n_q = n\,[RPM]\frac{\sqrt{Q[\frac{m^3}{s}]}}{H[m]^{3/4}} \quad (1)$$

The conversion factor between n_q in SI-Units and n_s in US customary units is 51.6.
The specific speed coefficient and the diameter coefficient are defined as follows:

$$\sigma = \frac{\varphi^{1/2}}{\psi^{3/4}} \quad (2)$$

$$\delta = \frac{\psi^{1/4}}{\varphi^{1/2}} \quad (3)$$

$$\text{with } \varphi = \frac{2*\Delta p}{\rho*2*\pi*n*r} \quad (4)$$

$$\text{and } \psi = \frac{current\ Massflow}{theoretical\ Massflow} \quad (5)$$

Where r is the radius of the impeller, Δp is the difference pressure between inlet and outlet and n is the rotational speed.
The Cordier diagram shows, an alternative with higher efficiencies to side channel pumps: displacement pumps. Quite often those PD pumps need high NPSHA values to run free from cavitation or their bearings have to be lubricated with oil or other contaminous

lubricants. Some of them are leaking through the piston packing, which limits their use with respect to volatile organic compounds (VOC), and usually a strong pulsation of the massflow is occurring. Whereas massflow-pulsation in side channel pumps is not appreciable and with using journal bearings by design, the pump is able to run free from impurity with the pumping liquid itself as lubricant for the bearing bushings.

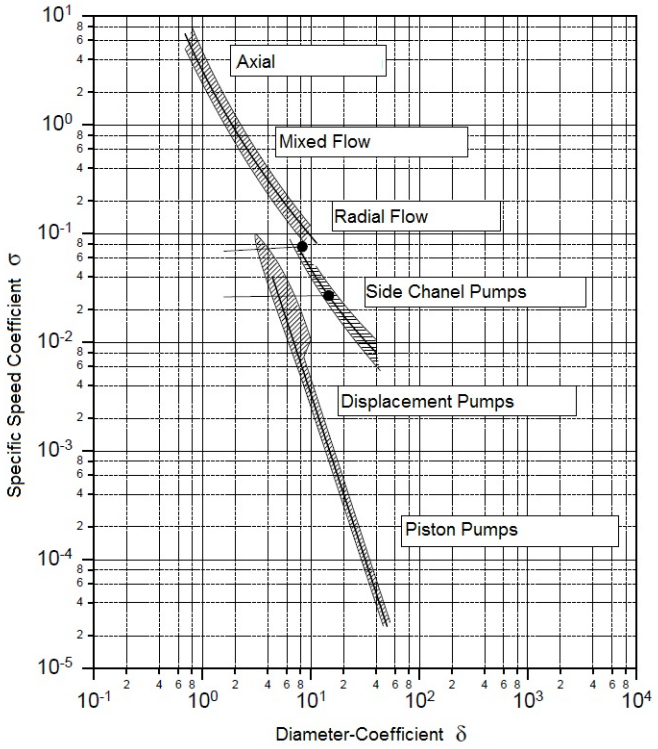

Figure 6: Cordier diagram with side channel pumps (Beilke 2005)

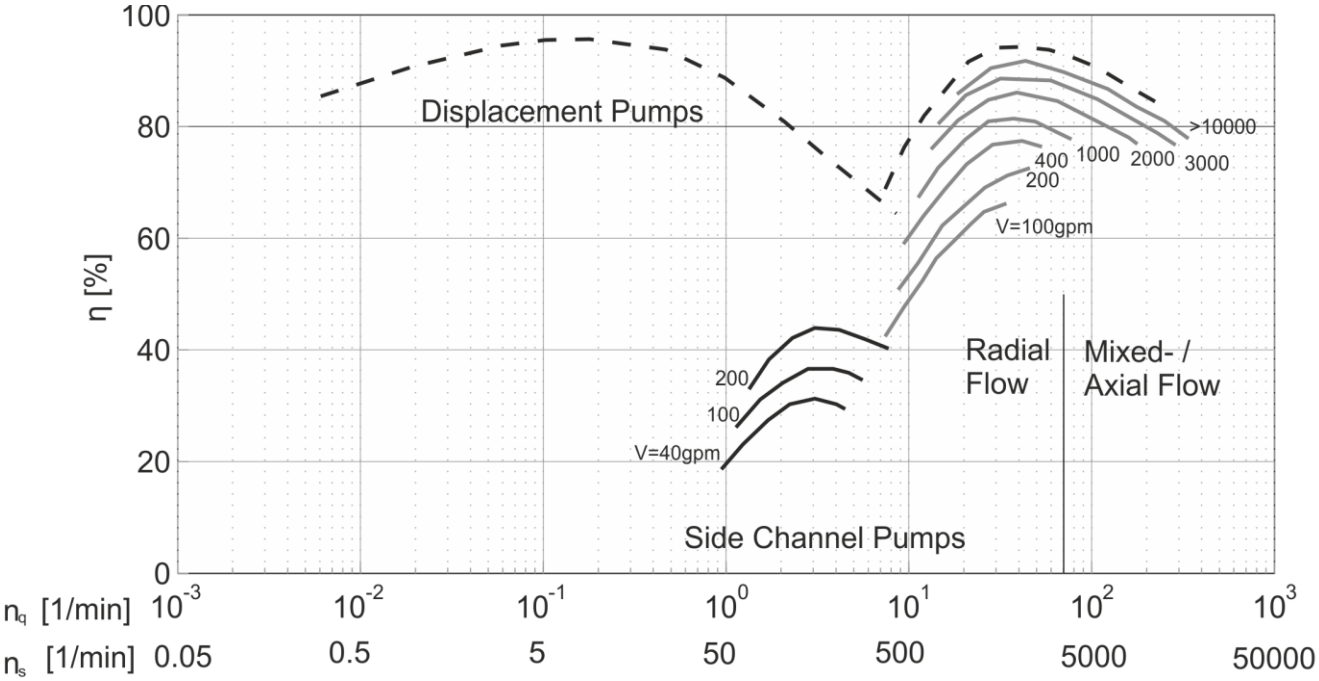

Figure 7: Maximum possible efficiency for different pump types (Fleder 2015)

PART TWO: PRELIMINARY INVESTIGATIONS

Preliminary experimental investigations

A newly developed multistage High Pressure Pump is used for the tests. The pump is available in one size but different number of stages. Eight stages is the maximum and the pump then produces heads of 3,700ft at a flow rate approx. 4.4GPM at 3600 RPM. The stage specific speed of the pump is n_q=12 (n_s=620). A cutaway of a three-stage pump with NPSH-1st stage and magnetic coupling is depicted in Figure 8.

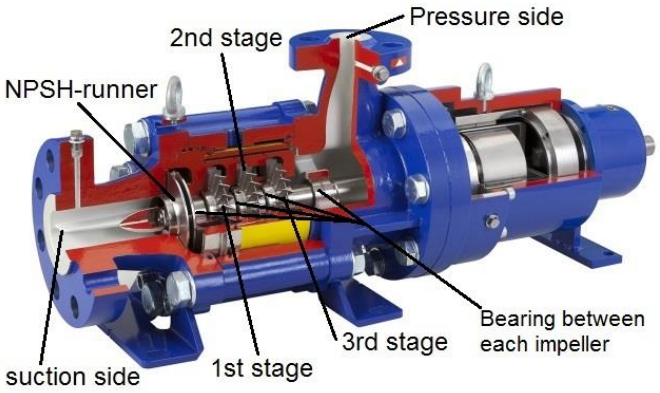

Figure 8: Cutaway of test pump

The pump is designed to run on 2-pole motors with natural speeds of 2900RPM (50Hz) or 3500RPM (60Hz) depending on the application, which is unusual for side channel pumps. Usually Side channel pumps run at 1800RPM or lower (4- or 6-pole motors at speeds of 1750RPM resp. 1150RPM). Due to the high rotational speeds and pressure differentials, the test pump impeller needs reinforced blades. A supporting ring is used preventing the blades from bending and also helps to guide the liquid. This ring is unusual for all side channel pumps.
The blades are set with a variable angle from the hub to the outer diameter to reduce the losses that occur during the interaction of impeller and fluid and to achieve maximum possible heads.

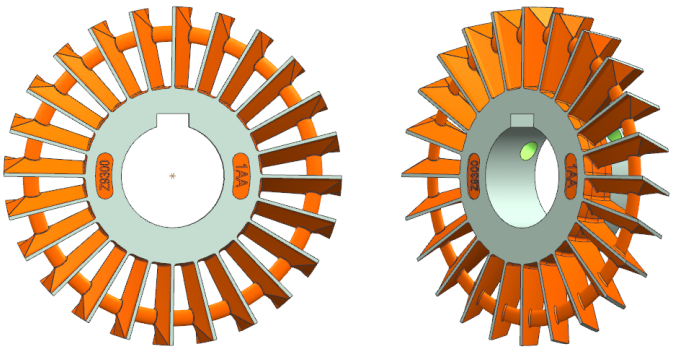

Figure 9: Impeller of test pump

Due to pressure limitations in the NPSH test circuit, a 3-stage pump with a head of 1050ft at minimum flow is tested. In comparison to Figure 8, the second side channel impeller is removed and an empty stage (blind stage) is assembled.
The pump is tested as two-stage version. To minimize the NPSH3% value of the side channel hydraulics, a classical radial impeller, named NPSH-impeller, is mounted at the suction end of the pump. As the head of the NPSH-impeller is small compared to the head of a side channel stage, it can be considered to describe the NPSH-1st-stage lowering NPSH at any speed without remarkable effect on the head and efficiency of the pump.
This assumption is based on the suction specific speed, which calculates in line with the specific speed but with NPSHR instead of

head. Suction specific speed for the test pump at 2900 RPM in BEP (26 gpm and 2.2ft NPSHR) is 7600 US, which is a quite high number. Below the BEP, the NPSHR is even lower, which can result in Suction specific speeds of 9000 US and higher – without bad influence on equipment availability.

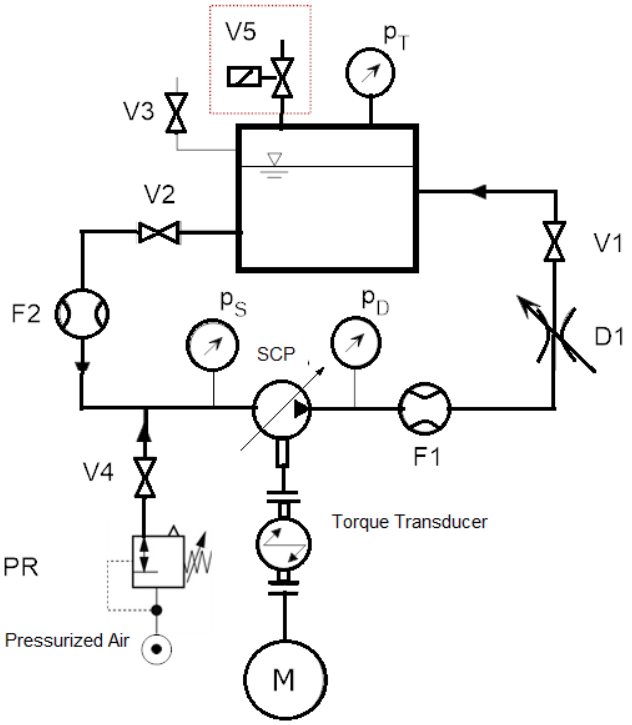

Figure 10: Schematic of the test rig for side channel pumps

Due to the mentioned limitations the performance curves could only be tested up to approx. 230PSI (16bar). A closed tank, able to provide over- or underpressure, is connected to the pump. At the suction piping, the volume flow and the pressure is measured. An additional dosing device to control gas volume-flow-rates allows testing of the gas handling ability in 2-phase flows (gas-water mixtures).
At the discharge piping pressure and temperature transducers were placed as well as a throttle valve to control the volume flow to allow setting a specific duty point. A simplified schematic of the test rig is depicted in Figure 10.
To ensure valid measurement, a sequence of data points is measured and averaged. Each characteristic curve is measured several times to provide reliable statistical data. The head curves for different nominal speeds from 2000 RPM to 3500 RPM as well as a comparison to the manufacturers head curve are shown in Figure 11.

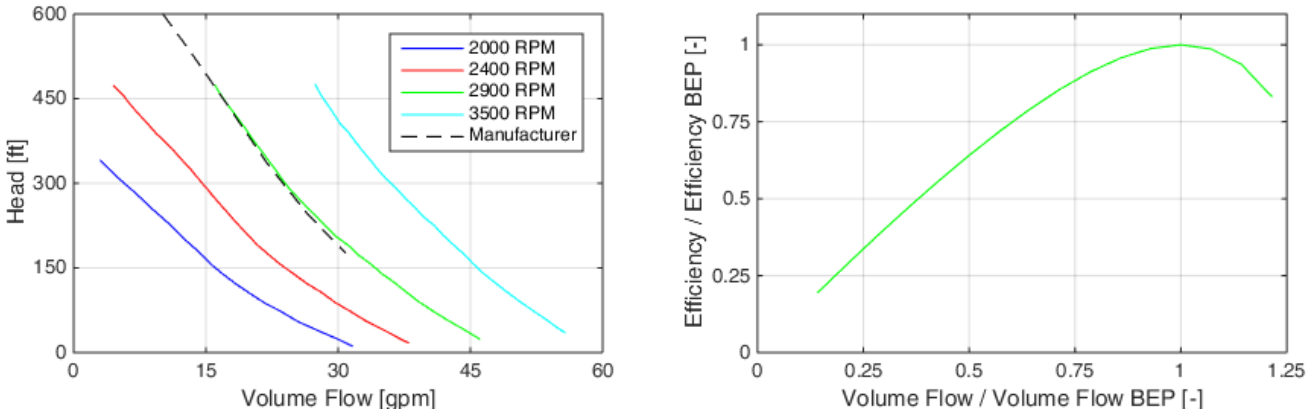

Figure 11: Characteristic curves for different speeds for the test pump

The head rises in a very steep curve from high flow rates to lower flow rates, with a tested maximum of 46GPM at 2900 RPM.
When applying the affinity laws for head and flow to the measured curves at different speeds, the curves are corresponding pretty good and are almost congruent. The BEP is located at high flow rates (about 38 gpm for 2900 RPM).
Figure 12 shows the NPSH3%-curve for the test pump. With rising volume flow, the NPSH value is rising slowly. At maximum flow rate of 40GPM, the NPSH-value reaches still low 4.4ft. At lower flows, values below 2ft are reached. Lower values cannot be measured at the test rig used for these series of tests, due to limitations of the vacuum pump and small leakage of the tank and the piping. With a different, optimized test rig for lowest values, 9" of NPSHR were measured before for a similar test pump running at 2900RPM! The dashed line in the following figure shows the experimental results determined at the optimized rig, which are also provided by the manufacturer for benchmark. As these measurements have not been performed by the authors, no detailed information on the test procedure can be given.

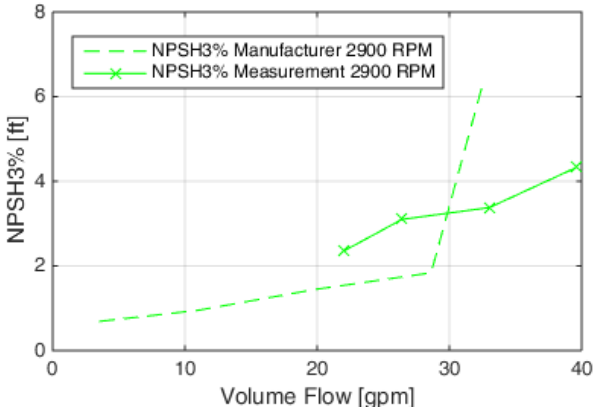

Figure 12: NPSH3% value for original pump

Determination of hydraulic forces for water and n-hexane
Numerical flow simulation

As the hydraulic forces that need to be compensated by the bearings are a result of the pressure distribution on the shaft and the impeller, the forces in all directions are pulsating. Impellers with fully radial, straight non-angled blades are often operating free of any axial force and therefore can be mounted axially free floating on the shaft. Most industrial (centrifugal) pumps are using impellers with angled blades and reinforcements on the back side. These are usually fixed to shaft, as the pressure distribution lead to an axial force. As the tip as well as the gap clearance between impeller and casing are the most important parameters in side channel pumps (gap size has a significant effect on characteristic curve), this parameters have to be considered at the assembly.
The numerical investigations are performed using ANSYS CFX 14.5. The meshes are blockstructured meshes only consisting of hexahedral elements for the impeller (two Million elements, 2.2 Million nodes) and the inlet and outlet area (200,000 elements). The side channel is meshed with a specially developed hybrid mesh, consisting of one million elements (420,000 nodes),, hexahedral and tetrahedral. Recent studies on the effect of the mesh size showed, that this size is appropriate for side channel pumps. The entire calculation volume including inlet and outlet tube is depicted in Figure 13. The fluid enters at the inlet from the left side, is moved in a spiral flow through impeller, consisting of 24 blades, and side channel and leaves the pump through the outlet on the right side.
The inlet boundary condition is set to a minimum total pressure (1Pa), a mass flow is set at the outlet. The working fluid is single phase water or hexane (viscosity = 1 cP or 0.3 cP, density 1000 or 700 kg/m³), both incompressible. The losses in the pump are expected to be not large enough to heat the fluid in a way that it changes its physical properties much. So the temperature also is set to a constant value. As the viscosity does not depend much on the pressure, it is set to a constant value as well.

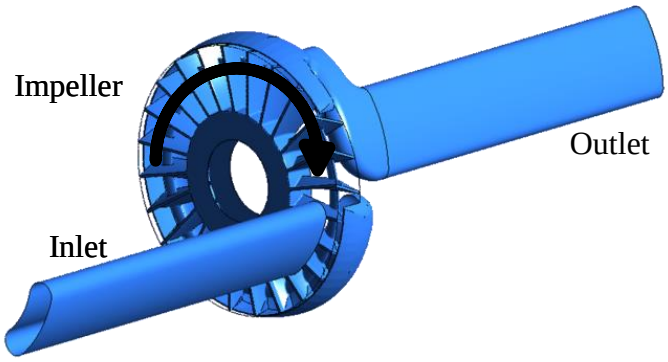

Figure 13: Domain of interest for numerical investigations (impeller rotation CW)

The connection between impeller and side channel is a transient rotor stator interface, as all simulations have to be performed transient. The time step between two calculations is chosen to rotational steps of 1° of the impeller. So at 3500RPM, the time step results in 4.762microseconds. At least 1080 steps, which correspond to three full impeller revolutions, need to be simulated, to ensure a valid and periodic result.
Outlet pressure, torque and forces are pulsating in a periodic manner. The width of the pulsations depends on the number of blades of the impeller. Every pulsation corresponds to one blade crossing the breaker area (approx. every 15°).

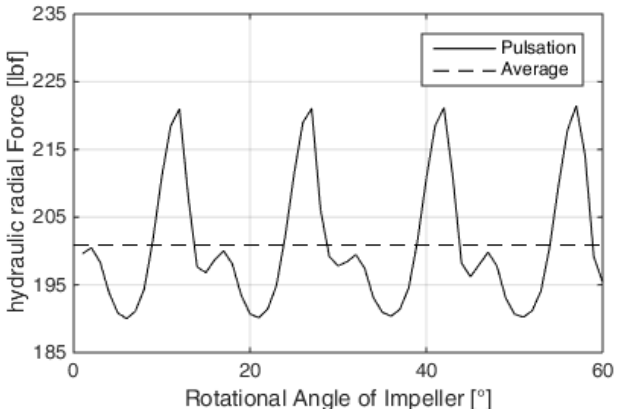

Figure 14: Pulsation of radial force

The resulting forces for a period of 60 timesteps (corresponding with 4 blade passages) with hexane as working fluid at 18 gpm (25% BEP) at 3500 RPM are shown in Figure 14 and Figure 15. The forces are mathematically evaluated in a rotating reference frame (Cartesian coordinate system).
Therefore, when summing up to a resulting radial force, the direction of the force varies with every time step. When seen from a stationary coordinate system (e.g. from the stage casing), the radial force always points to the same direction.

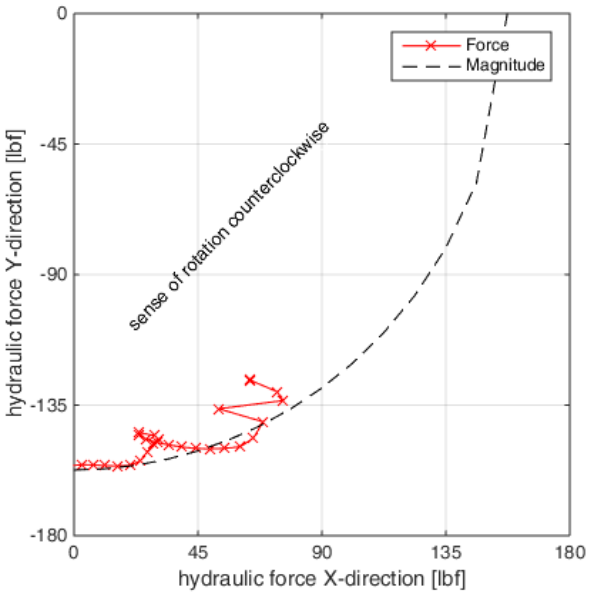

Figure 15: Hydraulic forces on the impeller in rotating reference frame

The pulsations are way less significant than in the outlet pressure. The static portion of the force is more than 90% of the peak value. Only 10% of the force is a transient pulsating part, generating a tiny pump effect in shaft micro movements.
In general, the pressure and therefore also the forces reduce when using hexane as a working fluid. With increasing head and decreasing volume flow, the radial forces increase as well. The maximum value is about 337 lbf (1500 N) for pure water and 225 lbf (1000N) for pure hexane. Figure 16 shows the force as function of the flow on hexane for different speeds.
Hexane was chosen as a pumping fluid because it is a good representative for hydrocarbons in the intended main application field of the high pressure test pump in fracking and other Hydrocarbon midstream processing applications. Hexane represents a low viscosity liquid (0.3cP) with low specific gravity. The hexane viscosity equals viscosity of water at 160°F, so this made it possible to evaluate the calculated load capacities of the bearing bushings avoiding a test loop with liquefied pressurized hydrocarbons (compare PART THREE). All other fluids (like ethane, propane and others) can be estimated with the results and tendencies of water and hot water / hexane results. The following table gives an overview of possible working fluids, all within the range of viscosity and density.

Table 1: Possible working fluids

	Vapor pressure	Specific gravity	Dyn. Viscosity	Kin. Visc.
Media	[PSI]	[-]	[cP]	[cSt]
Caustic (20/80)	0,6	1,15	2,2	1,91
Glycol (TEG @ 225°F)	5	1,12	35	31,25
Rich Amine	4,7	1,01	1,8	1,78
Water (68°F)	0,34	0,998	0,95	0,95
Water (160°F)	4,72	0,977	0,35	0,36
Light crude oil	0,01	0,85	10	11,76
Methanol	4,6	0,79	0,48	0,61
Hydrocarbon Condensate	6,4	0,65	0,38	0,58
Natural Gas Liquids (Y-Gr.)	170	0,5	0,25	0,50

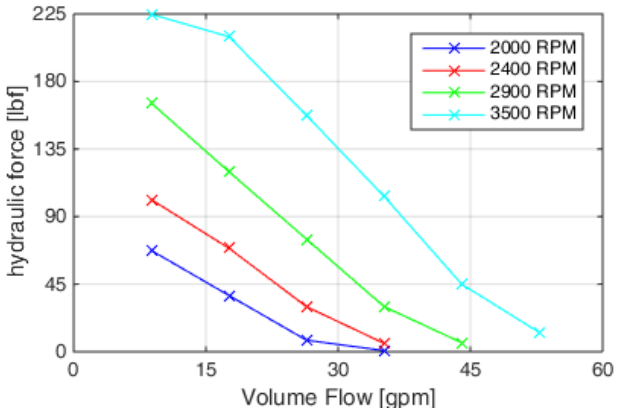

Figure 16: Hydraulic forces for a single pump stage with hexane

PART THREE: NUMERICAL INVESTIGATION AND TESTING OF JOURNAL BEARINGS

Numerical investigations of bearings

The numerical investigations are performed using ANSYS CFX 14.5, like for the simulations of the hydraulic forces. The gap of the bearing is meshed in 2D and then rotated by steps of 1°, resulting in a mesh with 360 cells in circumferential direction. The gap height is meshed with at least 10 cells. Rotor and stator are in a stationary reference frame although pulsating with micro movements, the rotor boundary condition is rotating wall. The simulations are steady state, with a moving mesh option. This means when performing a displacement, the mesh gets compressed and stretched automatically. The working fluid is water with constant temperature. The target criteria are the forces in the three directions. The simulation is stopped when target criteria and residuals are in a steady state.

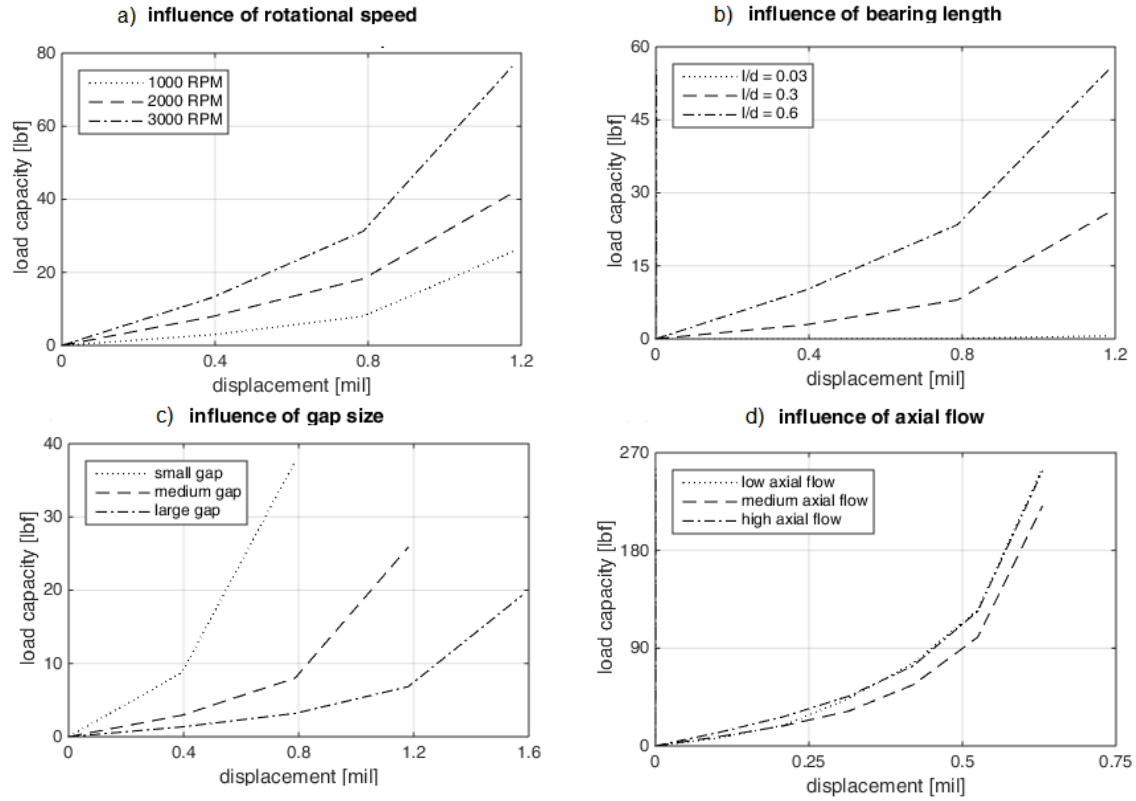

Figure 17: Influence of main parameters on load capacity, numerical results

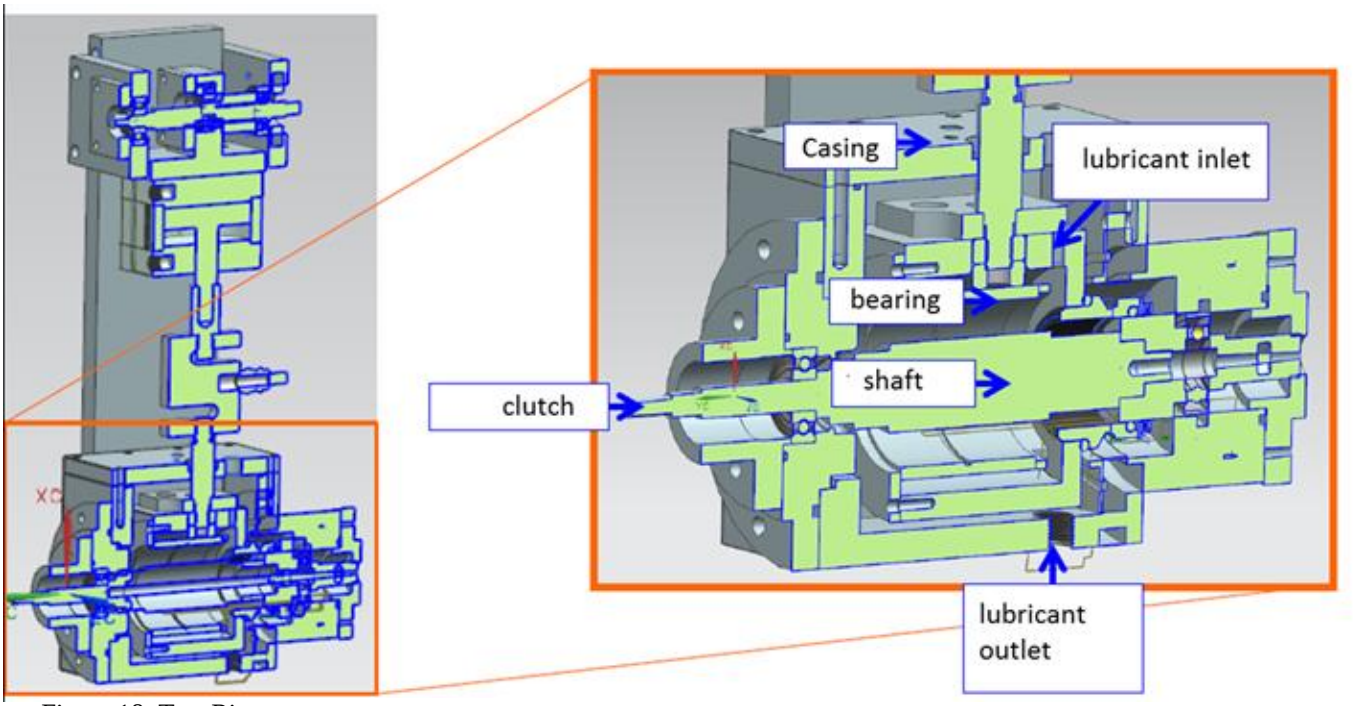

Figure 18: Test Rig

A large variety of journal bearings is investigated in numerical simulations, to identify the influence of geometrical and operational parameters on the possible load a bearing is able to carry. The simulated bearing sizes are 32mm of inner diameter (1.26 in) with gap sizes of 1 to 2 mil, and length/diameter ratios of 0.03 to 0.6.Pressure drops ranging from 1 to 6 bar, depending on the axial flow. Reynolds numbers are all located in the laminar flow regime below 200.

Figure 17 shows the influence of rotational speed (a), bearing length (b), gap size (c) and axial flow (d) (coolant / flushing) to the load capacity of a single bearing bushing. The results are later compared to theoretical design rules and the experimental values in a practical adjustment, to evaluate the best design.

With increasing rotational speed of the shaft, the load capacity of the bearing rises. A larger diameter, increasing length or a decreasing gap size also increase the load capacity. The axial flow of the flushing liquid itself has no significant effect and can therefore be neglected. It should only be considered for reasons of cooling to avoid thermal stress of the bearing.

The simulations are performed with the same CFD code as all others to allow a combined simulation of side channel stages with the bearings, means direct coupling of the hydraulic forces with the displacement of the shaft. These investigations have not been performed yet. Plain bearings have been chosen, as these are simple and easy to manufacture in a broad variety of different materials. Other, more sophisticated bearing designs like lobed geometries or the use of porous material for the bearing shell are possible in general, but not needed.

Test Rig and experimental investigations

Figure 18 shows a cutaway view of the test bench setup. The shaft is split in two parts, each supported by two ball bearings. Both shafts are connected with a screw. The part with the bearing surface is wetted and is sealed with a mechanical seal. The shaft is connected to a motor with a coupling.

The bearing bushing itself is installed in an adaptor. A maximum of 281lbf of force can be applied by an air operated pneumatic cylinder connected to a load cell acting via a push rod to the bearing housing in radial direction towards the bearing bushing. So in the setup the shaft is rotating but radially and axially fixed; the bearing bushing is allowed to move in any radial and (to some degree) axial direction.

Bearings in four different sizes were manufactured, which allow proving the influences identified in the numerical investigations. The bearing sizes are shown in the following Table 2.

Table 2: Bearing size overview (metric dimension)

Bearing Name	Inner Diameter (shaft)	Outer diameter (bearing)	Bearing length
35025	35 mm	35,025 mm	35 mm
4004	40 mm	40,04 mm	40 mm
4006	40 mm	40,06 mm	40 mm
4505	45 mm	45,05 mm	22 mm

Each bearing was installed in the test rig and tested with different speeds. For every single test, the speed was set and force was applied. The force automatically rises with time. Where possible, the maximum force was applied. In many cases, the bearing came very close to the shaft and starts to run with some measurable stick-slip effect, because the minimal useable bearing clearance was underrun and the lubricant couldn't fill the gap any longer. This effect was detected and observed by a significant, rapid increase of drive power. The drive power was determined with the measured motor current, depicted in Figure 19 for a bearing of size 40x40.06x40 mm. At a radial load of approx. 83lbf for the speed of 1100RPM, the drive power is about 25 times higher than at the beginning. This point indicates a beginning material contact at certain points and areas of the surface, which goes hand in hand with wear and abrasion. Sooner or later this overload will lead into a worn out bearing bushing.

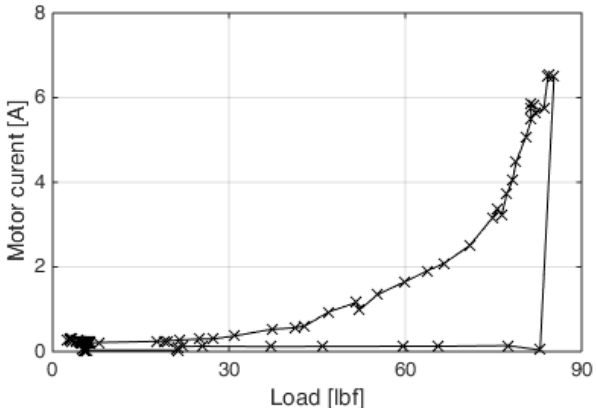

Figure 19: Motor current over a rising load, experimental result (1100 RPM)

Figure 20 shows the experimental results for the bearings designed previously, compared to the value of the maximum load capacity following the theoretical design criteria, described in the appendix. A good accordance between the theoretical and the experimental load could be found. The experimental values are within 10% of the theoretical values.

Maximum load capacities increase with the rotational speed of the bearing for all sizes. This behavior was predicted by the numerical investigations and the theory and can be validated. An increasing bearing size does not necessarily increases the load capacity; it was found, the combination of diameter and clearance defines the load.
It is possible to calculate the load capacity for pure hexane as lubricant, based on the theoretical values. This recalculation of the results to hexane as a pumping liquid does not change the trends of the load capacity as function of the rotational speed. Only the absolute maximum load is reduced. The same bearing can carry a load of 90 lbf (400 N) for water, but only 30 lbf (135N) for hexane, justified by the lower viscosity of hexane. The recalculated theoretical values can be seen in Figure 21.

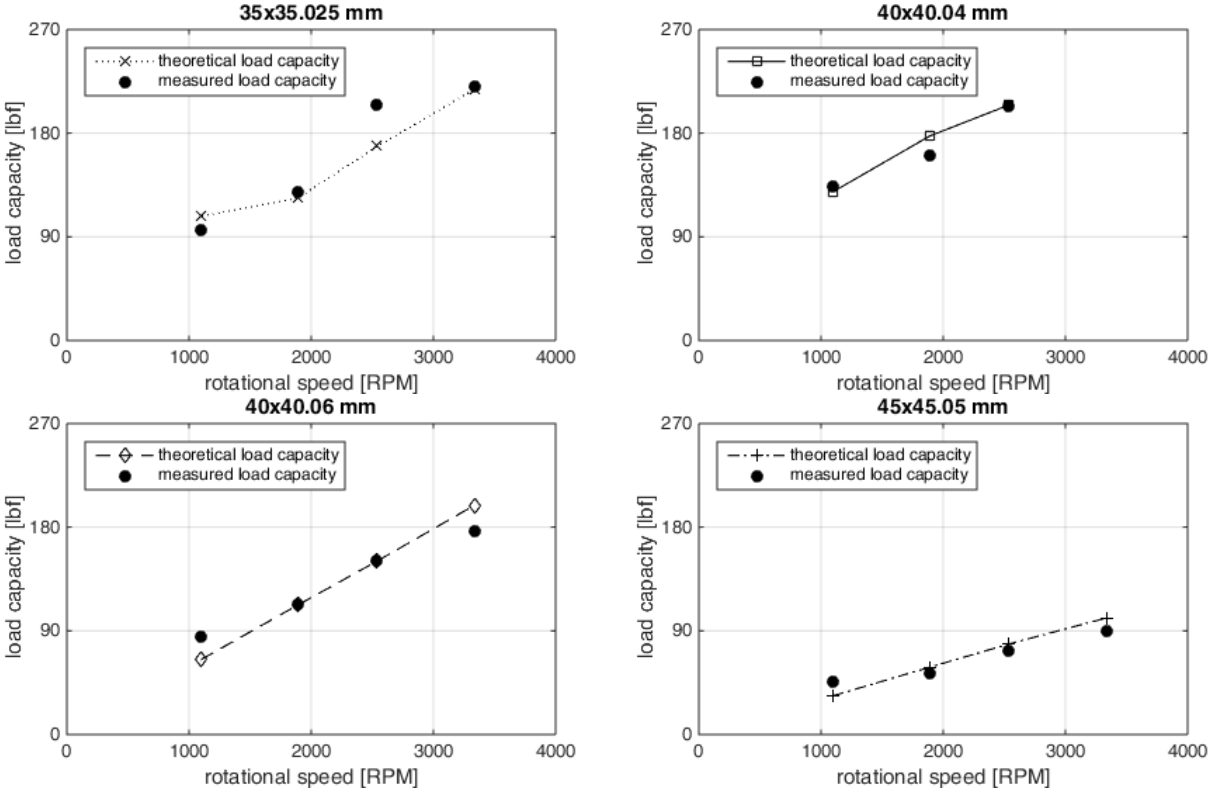

Figure 20: Load capacity of journal bearings for water, experimental results

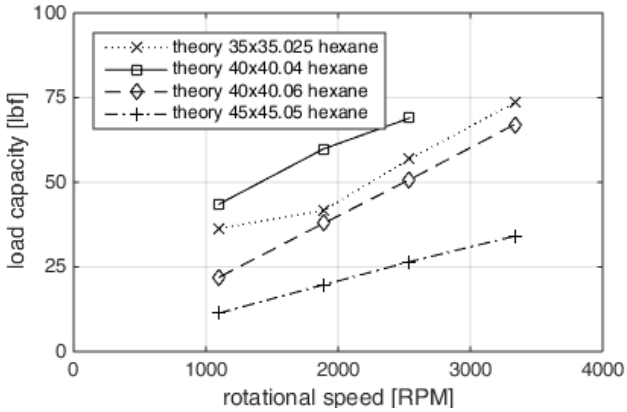

Figure 21: Load capacity of journal bearings for hexane, scaled values of the theoretical values

Design of Bearings for the pump

Most critical applications were found in the performance range, when the pump runs in (extreme) part load at high speeds. Low flows and high heads result in high radial forces.
To reduce the sheer size of the bearings to allow a much more compact stage assembly, some design measures to reduce the load are applied.
To find the most critical assembly, a schematic of the pump is analyzed and the load of every stage is summed up, respecting the individual direction. The number of similar bearings in the pump is always "number of stages"+1.For reasons of best fluid flow with smooth guidance and reduced pressure-losses in the pump, every stage is twisted by an angle of 52° to the previous one. Therefore the radial force of the second stage is pointing in another direction – to be specific: twisted by the same 52° to the force of the first side channel stage. The third stage then is twisted by 104° to the first one and so on. Radial forces of the side channel stages from the first

to the last are twisting gradually (0°-52°-104°-156°-208°-260°-312°-364°). Due to the small axial interspaces (1.5") from one bearing bushing to the next and the shaft diameter (1.26") in relation, the radial forces (incl. weights of shaft and impellers) are partly compensated one below the other. Figure 22 shows the maximum load capacity of different bearing sizes in relation to the fragmented radial forces per bearing bushing with varying number of stages for hexane and water.
The twisting angles for variable twist are depicted in Table 3

Table 3: variable twisting angles

No of stages	Twisting angle of special stage
2	180°
3	154°
4	128°
5	102°
6	76°

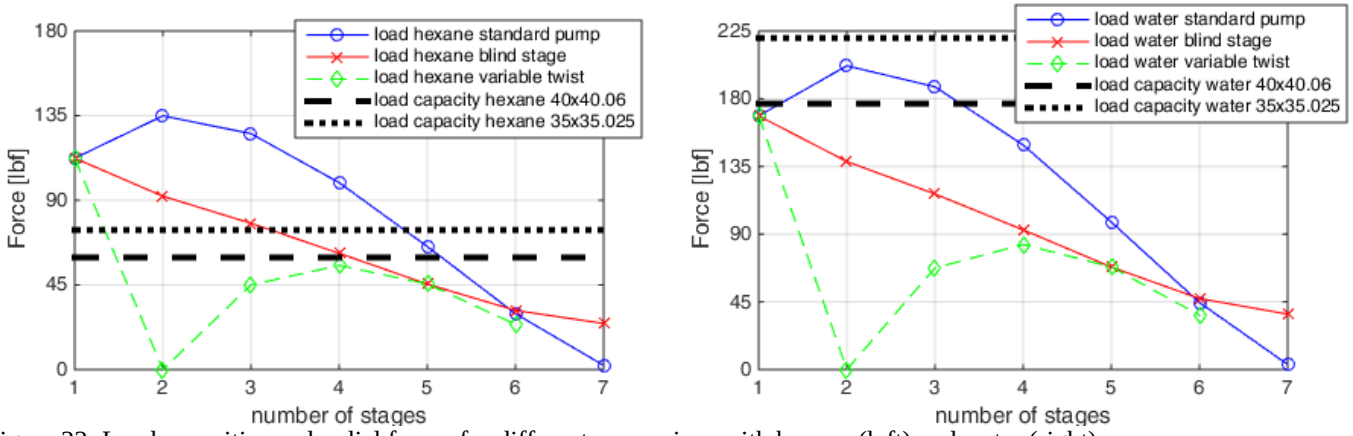

Figure 22: Load capacities and radial forces for different pump sizes with hexane (left) and water (right)

For example: The maximum load each bearing has to carry is calculated to 200 lbf for water and 136 lbf for hexane for a standard pump with two stages, and a slightly lower load for a pump with three stages.
One way to reduce the load per bearing by design is to modify the twisting-angle. One simple trick is by adding an empty stage without impeller (blind stage) as second stage, but twisted as standard. Thus the twisting angles of all following stages are automatically increased by 52°. Now, the load can be reduced from 200 to138 lbf on water (136 to 92 lbf on hexane) per bearing for the two-stage pump and to 116 lbf (77 lbf on hexane) per bearing for the three-stage pump. For a higher number of stages, the radial forces decrease as well or stay at the same low level.
With the maximum load capacity of two representative bearings (35.025 and 40.06) shown in the figure, it can be read that the smaller bearing is able to carry the load for all pump sizes when water (at 70°F / 1cP) is pumped, no matter if the stages are additionally twisted or not. When pumping hexane, the pumps with four or lower stages are critical in the standard setting. Additional twisting of the second stage with the use of a blind stage results in only one- and two-stage pumps could come into trouble depending on the flow rate and resulting radial force.
By adding a specialized blind stage even a complete compensation of radial forces in the specific pump is possible. Therefore a variable twisting angle is adjusted to optimize the force distribution and minimize the load per bearing. It is now shown, that pointed radial forces in a multistage side channel pump can be used to self-compensate the radial thrust.
The bearings themselves are possible in carbon or silicon carbide material. Second prolongs lifetime of the pump if in intermittent mode with numerous switching operations per hour. It is advisable to combine silicon carbide bearings with a hard faced shaft to get maximum bearing gap stability and minimum wear, see Figure 23.

Figure 23: Silicon carbide bearing bushings w/ hard faced shaft

PART FOUR: NPSH-IMPELLER

As mentioned before, one of the main targets for the new pump is the hydrocarbon processing industry (HPI), such as mid-stream (fracking) gas processing applications. Very often low viscosity fluids are handled close to their individual vapor pressure ⇨ NPSHR < NPSHA is a MUST for successful operation. As the low specific gravities of the handled hydrocarbons do not generate much of a natural NPSH at the geodetic height of typical on-site installations, there are only a few options. Generating artificial NPSH (by chilling or pre-pressurizing the liquid) is expensive. Vertical can pumps are a viable way, but for low flows the achievable efficiencies are quite often in the single digit range. High pressure side channel pumps are a true alternative for lowest flows.

As depicted earlier in Figure 12 the NPSH3% value is rising from 9" at min flow to 2ft at moderate flow rates of 23GPM and then to values of over 4.4ft at high flow rates of approx. 45GPM. So for higher flow rates, this effect has an increasing importance for successful operation.

Main influence on the NPSHR of the entire pump unit is from the generated head and the very own NPSHR of the NPSH-impeller in front of the side channel stages. As the head is small in comparison to the head of the side channel stages, the NSPH-impeller is considered as low-NPSH-stage and not as the first pump stage. Therefore, the NPSH3% value is evaluated as the 3% drop in head of the first side channel stage. The head of the NPSH-impeller is about 15% of the head of a single side channel stage at flow rate of 10 gpm and slightly higher at higher flows. The arithmetical portion of the NPSH-impeller in regard to the generated head decreases to 2 to 3% in an 8-stage pump at the same flow rate. Suction specific speed for this design at BEP of the side channel stage (36gpm) is very high, so even it is a radial impeller, the suction specific speed is relatively high and legitimates the assumption of an inducer-like function, which allows to determine the NPSH3%-value as the pressure drop of the first side channel stage instead of the first pump stage, which would otherwise be the NPSH-impeller.

A side channel pump without NPSH-impeller has much higher NPSH3%-values. At maximum flow, in the overload region, the NPSHR can easily reach 30ft and higher, which means that those pump configurations are good for applications with very high suction pressure and a comfortable margin to the vapor pressure.

A new NPSH-impeller was designed with the focus on the higher flows where the old one was a little weak. With modern CFD some slight improvements were achievable. To improve the NPSHR of the entire pump, it is assumed, that an improvement of the NPSH value of the NPSH-impeller itself improves the value for the whole machine. The design of the new impeller is performed following the procedures described in Gülich (2004), Troskolanski (1976) and Pfleiderer and Petermann (1991). These procedures have been found to deliver reliable results. General advice for the design of low-NPSH 1st stage is a large suction diameter and low number of blades. These advices are respected and a new impeller is manufactured, depicted in Figure 24. The spiral case and all other components stay untouched. First parts for testing purpose were produced in 3D- rapid prototyping and tested hydro-dynamically in the test rig.

Figure 24: New NPSH-impeller manufactured with rapid prototyping

As the result of modern rapid prototyping is precise geometry of the ideal calculated shapes, the question is, which impact the manufacturing (casting) process has on the results. The original impeller therefore was manufactured using two different casting techniques - sand casting as the traditional way to manufacture closed impellers (with two shrouds) and investment casting. These two impellers were compared with a new design impeller, using CFD in respect of the design regulations for low NPSH values, manufactured in plastics, using rapid prototyping.

Main goal for the new impeller is to provide a geometry that is easier to manufacture and less critical for small errors in the geometry. Therefore, the blades are chosen to be less distorted and with a uniform thickness. The original blades are twisted three-dimensional. To improve the performance of the new impeller in the operating range of the side channel pump, higher blade number is chosen (7 blades at new design, 5 blades at original design), as this improves the fluid guidance in part-load operation. The higher number of blades theoretically leads into blockage problems, but at such low flows it is assumed being not significant. The blade angle and suction eye diameter were expected to have larger influences. Nevertheless, a study of positive effect of lower the blade numbers should be performed. Therefore, an impeller design with additional splitter blades is taken into account. The negative effect of the higher blade number can be observed at higher flows beyond the operating range of the pump, so with no bad influence on the pump in reality. Inlet and outlet diameter stay the same, but the overall length (axial extension) is higher for the new impeller. This allows a smoother re-direction of the fluid. The cross section of the two impellers can be seen in Figure 25, new design on the top, the original geometry below.

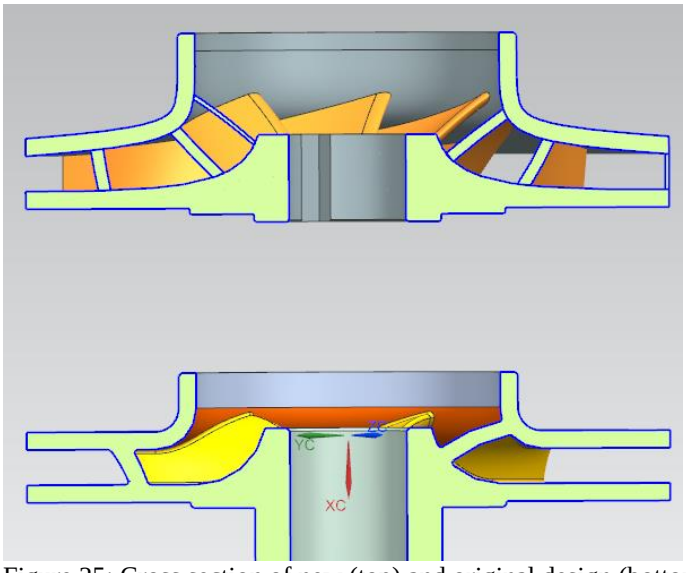

Figure 25: Cross section of new (top) and original design (bottom) impeller

The impeller is designed for BEP of 66 ft (20 m) at 44 gpm (10 m³/h) at 3500 RPM, as this is the minimum pressure the impeller must provide to prevent the side channel stage from cavitation. No specific target for NPSH3% has been set, but the goal was to evaluate the design and manufacturing aspects and check if rapid prototyping material is suitable for prototyping tests in high speed side

channel pumps, as basis for future developments and redesigns if needed.

Figure 26 shows the experimental results for head, efficiency and NPSH3% curves for the three different impeller, measured on the test rig depicted and described previously in Figure 10.

The new designed impeller shows a slightly higher head in the entire operating range. The maximum head is 75 ft (23 m) at 4.4 gpm (1 m³/h), the maximum flow rate is about 80 gpm (18 m³/h) at 30 ft (9 m) head. The design point of 66 ft (20 m) at 44 gpm (10m³/h) is almost hit. The two original impellers show a difference of about 3,5 ft (1 m) in head between each other and an additional 1,5 to 3.5 ft (0.5 to 1 m) in the operating range of the side channel pump (up to 53 gpm / 12 m³/h). The efficiency – minor important, as the impeller only works as a pressure-increase to lower NPSH-value for the side channel stage – is at a maximum of 55%, in comparison to 53% of the original impeller.

The NPSH value with the new impeller at 44GPM equals the original ones, but has a steeper slope to higher flows. This increase is an effect of the higher blade number. To lower flows the new impeller was tested to be slightly better (1 to 2"), than the old ones, which is an important step towards improving NPSH3% for low flow applications. Flows higher than 40GPM typically don't appear with this size and pump type, designed for high differential pressures.

Besides the slight improvements for NPSH, head and efficiency of the new impeller design, more important was the discovery of the significance in the manufacturing process of the raw parts. Outer dimensions of the NPSH impeller are machined of course, but the internal geometry of the blades and shrouds - beginning in the suction mouth and ending at the individual tips of the blades – remain for the most part in their casted quality.

It is demonstrated, that the traditional sand casting process has no satisfactory outcome even if more expensive ceramic cores were used during the casting process. The extreme NPSH values, which are achievable in this extreme flow range, need some unconventional methods to guarantee precise geometries with the casting process. Such were found in the investment casting with the lost wax pattern. Ovalized leading edges on the blades to allow loss-free inflow, sharp-edged intersections between blades and shrouds and perfect beveled blades' tips are possible with extraordinary smooth surfaces to minimize friction losses.

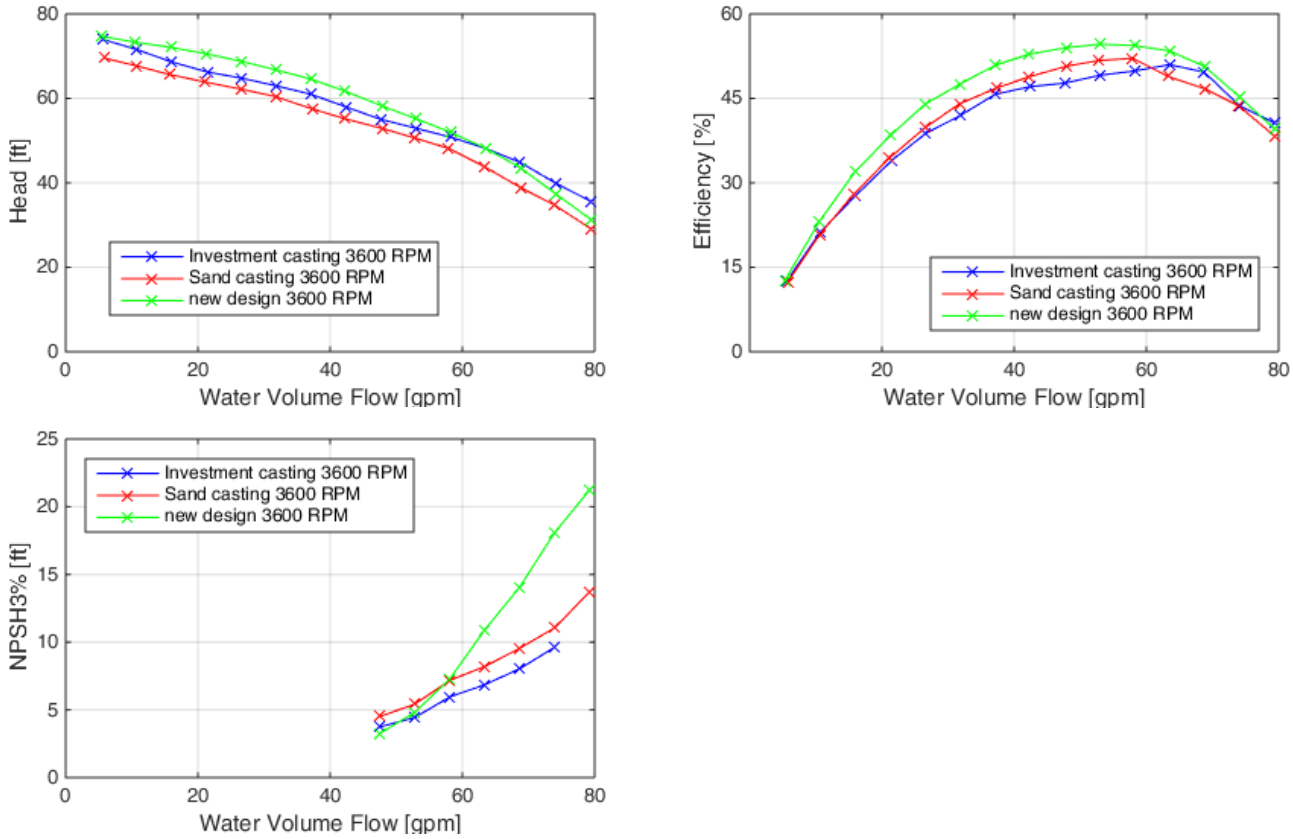

Figure 26: Characteristic curve and NPSH-value for NPSH-impeller

It must be stated that large differences between the two casted impellers are observable. Taking into account that they are

manufactured using the same geometry, the influence of small differences with the reproduction in the casting process is significant. Figure 27 shows some differences in result of two casting technologies.

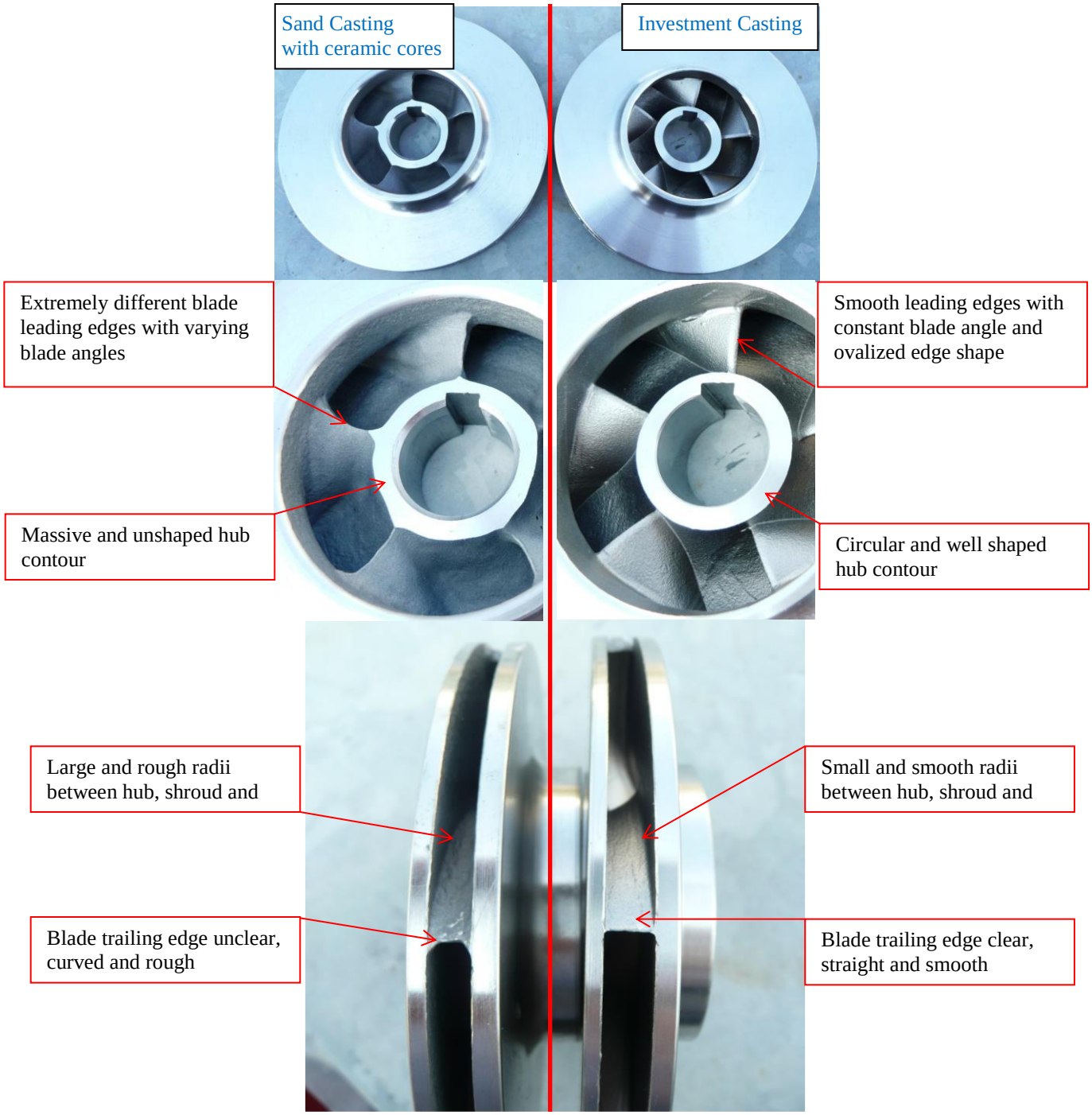

Figure 27: Optical comparison for different casting technologies

CONCLUSIONS

To use of rotodynamic multistage pumps like the side channel pump with hydrocarbon processing applications, especially for the low viscos, lightweight liquefied gases and condensates, some special provisions have to be considered within the pump design to result in durable and reliable equipment.
First, the design of the journal bearings.
The classical design regulations were applied for low-viscosity fluids and are appropriate. Main parameters are identified and validated in numerical investigations. A reduction of gap size and increase of the length are the parameters with the biggest impact on the bearing load capacity. The influence of the axial flow through the bearing can be neglected for the load capacity, but should be validated for lubrication and cooling purposes. Numerical investigations show the main influences of bearing design parameters on load capacity. The test rig proves the trends and values of the designs and numerical investigations.
The radial loads in side channel pumps can be very large, but the radial load per stage is directed relating to the side channel geometry. A way to reduce the loads by design is shown and applied in combination with new bearings. When twisting the second stage to the first stage by adding an empty casing, the load can be reduced by 30% in the most critical region of the performance curve. A variable twisting angle with a specialized casing can reduce the radial loads even to a cumulative load of 0 lbf; so compensated completely. As the radial load is dependent on the differential pressure through pump and therefore the head, it can be suitable to assemble a pump with more stages than required as a minimum but running it at a lower speed reducing radial forces. No unique bearing combination suitable for the entire performance range and the variety of liquids could be found. An accurate knowledge of the radial loads at the duty point with the media properties is required to select the right stage and bearing setup. Journal bearings with coated surfaces or solid silicon carbide bearings together with hardened shafts can reduce the wear and improve the durability of the pump as well as the hardened surface is resistant against abrasive fines entering the gap (bigger particles, like sand, have to be filtered out anyway, due to the small running gaps of the SC impellers).
Second, the gas handling ability.
With any upset mode possibly liquefied gases are flashing (partly). Gas handling and mixed-mode operation has been explained with an analogy of self-priming. The pump type itself shows lower negative effects of entrained gas or vapor than typical centrifugal pumps operating in a similar range of specific speed.
Third, the NSPHR of the pump unit.
To prevent cavitation (and also permanent flashing of liquefied gases) in the pump, it is needed NPSHA > NPSHR. With lightweight hydrocarbons pumped “on the vapor pressure curve” a minimized NPSHR is essential. The NPSH-runner is tested separately, to analyze the risk of cavitation. A new runner is designed and tested in comparison to the old ones, manufactured in different casting technologies. The way of casting is very important for the accuracy of the geometry. Small differences such as unsharp edges or bigger radii on the blades show an influence on the NPSHR, the head and efficiency curve. With the unconventional* investment casting (*for closed impellers) and an improved impeller geometry, the NPSHR can be reduced to as needed, allowing an easier and more economic application by the customer. Dependant on what operating range is needed, a NPSH-runner with minimized NPSH3% values for lower or higher flows can be selected. The NPSH-impeller manufactured in Radpid-Prototyping are suitable to perform tests at nominal speed, without the need of applying affinity laws. This possibility reduces the cost of prototyping drastically.

The results of the presented investigations can be applied to all forms of side channel pumps with a large variety of applications. SCP, especially operating at high pressures with possible presence of gas at low NPSHR, are already successfully used in many applications such as listed in Table 4, providing a technical and economic benefit for the user compared to other pump types. The results can now enlarge the field of application to more extreme duty points with even higher pressures at lower flows, opening a larger field of application to the side channel pump type and improving the reliability and durability.

Table 4: reference applications for SCP

Application	Media
Condensate Recycle Pump	HC condensate
Re-run Pump	NGL
Compressor KO-Pump	HC + water
Amine Reflux	Amine
Glycol injection	TEG
Methanol injection	Methanol
Methanol removal	Water
De-Ethanizer sump pump	C3+
De-Propanizer sump pump	C4+
Reactor feed pump	Ethyleneoxid
Refrigeration pump	R-134A
Ammonia injection (SCR)	Ammonia
Carrier Gas Booster	HC

NOMENCLATURE

SCP	**= Side Channel Pump**	
NPSH	**= Net Positive Suction Head**	
RPM	**= Revolutions per Minute**	
d	**= Diameter**	**(L)**
n	**= rotational speed**	**(T^{-1})**
ω	**= angular speed**	**(T^{-1})**
U	**= surface speed**	**($L\ T^{-1}$)**
So	**= Sommerfeld Number**	**(-)**
A	**= Area**	**(L^2)**
r	**= Radius**	**(L)**

FIGURES

APPENDIX A

Design of Journal Bearings following DIN 31652-1:2015-06

The radial force determined by the numerical investigations is used to design the journal bearings. In general, a bearing is designed by dimensionless parameters, taking into account the fluid, the geometrical and operating parameters and material parameters from the bearing material. A bearing is schematically depicted in Figure 28.

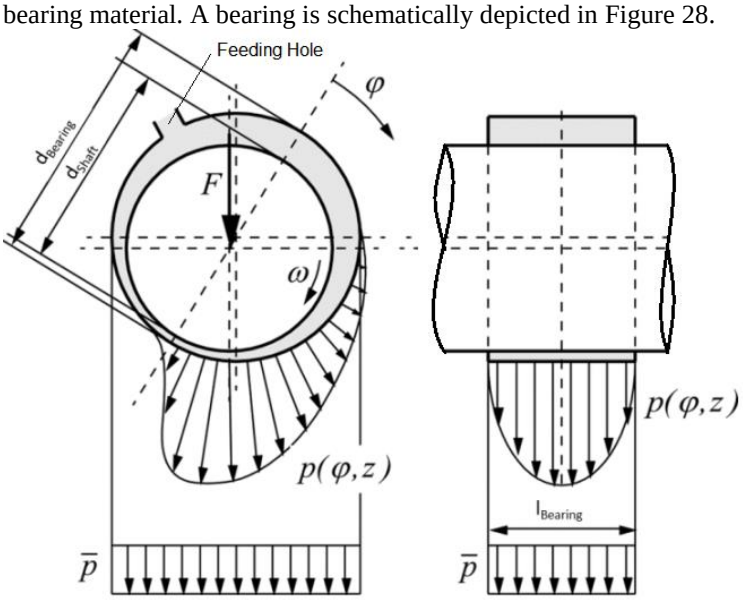

Figure 28: Schematic of a journal bearing, (Hoepke et al, 2015)

Table 5: Parameter grouping for journal bearings

Geometrical Parameter	Bearing Diameter	$d_{Bearing}$ [mm]	Resulting from Geometrical and Operating Parameters	Relative gapsize	$(1-\epsilon)[-]$
	Shaft Diameter	d_{Shaft} [mm]		Absolute bearing clearance	$h_0[\mu m]$
	Bearing Length	$l_{Bearing}$ [mm]		Useable baring clearance	$h_{o,available}$ [μ m]
Operating Parameter	Rotational Speed	n $[min^{-1}]$		Bearing pressure	$p_{bearing} = \frac{F}{l \cdot d_{bearing}}$ $[\frac{N}{mm^2}]$
	Angular Speed	ω $[s^{-1}]$		Relative bearing clearance	$\psi = 0.8 \cdot U^{0.25}$ [-]
	Sliding Speed	U $[\frac{m}{s}]$	Stability Parameter	Sommerfeld Number	$So = \frac{p_{bearing} \cdot \psi}{\eta \omega}$ [-]
	Force	F [N]		Relative eccentricity	ϵ via diagram (Sommerfeld number and l/d needed)

Table 5 gives an overview over the parameters used and calculated to design a bearing.

All geometrical and operating Parameters except the force can be chosen independently and define the bearing and all other dimensionless parameters.

The sliding speed and bearing diameter define a useable bearing clearance which should not be undercut to assure safe operation of the bearing. The bearing pressure is needed to choose the right material which is robust enough to resist the stress. For a given or guessed force, Sommerfeld number and relative eccentricity can be calculated. The result of both, together with bearing length is a clearance that will be present in operation. If this clearance is smaller than the useable bearing clearance, the bearing is unsafe and it exist a high risk of material failure and destruction of the material.

When designing a bearing for the pump with the desired load, a variety of different bearings with different diameters, lengths and clearances can be found. When a design has been found, the available space and other constructive reasons in the pump decide which bearing is used.

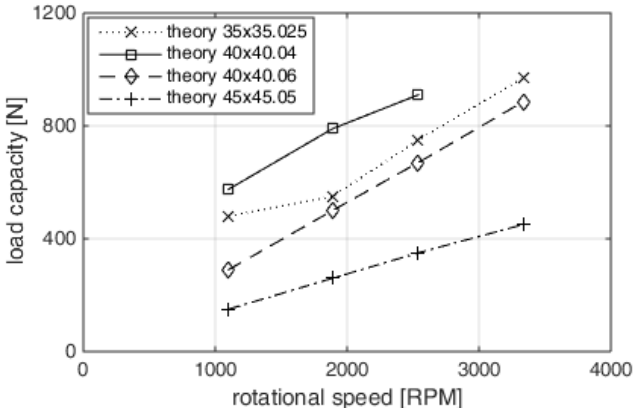

Figure 29: Maximum load for the designed bearings for pure water, following the DIN 31652-1:2015-06

Figure 29 shows the maximum load when designing a bearing following the instructions explained above. With an increasing rotational speed, the maximum load increases. Four different bearings are designed and manufactured after a numerical influence study.

REFERENCES

Beilke, J. (2005), *Numerical investigations on transient flow inside side channel blowers,* PhD, TU Bergakademie Freiberg, Dresden 2005, *(in Germany: Numerische Untersuchungen zur instationären Strömung in Seitenkanalverdichtern)*

Böhle, M. and Müller, T. (2009), *Evaluation of the flow inside a side channel pump by the application of an analytical model and CFD*. ASME 2009 Fluids Engineering Summer Meeting

DIN 31652-1:2015-06 (2015), *Plain bearings- Hydrodynamic plain journal bearings under steady-state conditions- Part 1: Calculation of circular cylindrical bearings*

Fleder, A. (2015), *Numerical and experimental Investigations on the influence of important geometrical parameters on the performance of side channel pumps taking into account the flow losses,* PhD Technical University of Kaiserslautern, Germany, Publisher Prof. Dr.-Ing. Martin Böhle, Shaker (in Germany: *Numerische und experimentelle Untersuchung des Einflusses wichtiger Geometrieparameter auf die Performance von Seitenkanalpumpen unter Berücksichtigung der Strömungsverluste)*

Fleder, A. and Böhle, M. (2012a), *A Study of the Internal Flow Structure in a Side Channel Pump.*Isromac 14, Honolulu, HI, USA

Fleder, A. and Böhle, M. (2012b), *Numerical and Experimental Investigation of the Influence of the Blade Shape of Industrial Side Channel Pumps* .International Rotating Equipment Conference 2012, Düsseldorf, Germany

Gülich, J.W. (2004), *Centrifugal Pumps,* Third Edition, Springer Verlag, Berlin 2014

Hoepke, B. , Uhlmann, T., Pischinger, S., Luedecke, B. Filsinger, D. (2015), *Analysis of Thrust Bearing Impact on Friction Losses in*

Automotive Turbochargers, ASME Journal of Engineering for Gas Turbines and Power, 137(8), August 2015

Lehmann, W. (1990), *Centrifugal pumps for special suction applications, reducing cavitation damage*, Kontakt und Studium, Konstruktion, Band 193, Ehningen 1990, *(in Germany: Kreiselpumpen für besondere Sauganforderungen; Vermeiden von Kavitationsschäden*

Lehmann, W. and Fandray, P. (1992), *Influence of hydraulic and geometric patrameter on the two-phase handling of side channel pumps for water-air mixtures*, Pumpentagung Karlsruhe, Sektion B1 Verfahrenstechnische Anlagen, Fachgemeinschaft Pumpen im VDMA Frankfurt, Karlsruhe 1992, *(in Germany: Einfluss hydraulischer und geometrischer Parameter auf das Förderverhalten von Seitenkanalpumpen für Luft/Wasser-Gemische)*

Pfleiderer, C. and Petermann, H. (1991), *Fluid Machinery*, Springer Verlag, Berlin 1991, (in Germany: *Strömungsmaschinen*, 6. Auflage)

Ritter, C. (1930), *On self-priming centrifugal pumps and experimentals studies on a new pump concept of this type*, PhD TU Dresden, Germany. *(in Germany:Über selbstansaugende Kreiselpumpen und Versuche an einer neuen Pumpe dieser Art*.

Schmiedchen, W. (1932), *Investigations on centrifugal pumps with side channel*, PhD TU Dresden, Germany , *(in Germany: Untersuchungen über Kreiselpumpen mit seitlichem Ringkanal*.

Surek, D. (1998), *Influence of blade geometry on head curve slope of side channel pumps*, Forschung im Ingenieurwesen 64, *(in Germany: Einfluss der Schaufelgeometrie auf den Kennliniengradienten von Seitenkanalmaschinen)*

Troskolanski, A. T. (1976), *Centrifugal Pumps, Calculation and construction*, Birkhäuser Verlag, Warschau 1976, (in Germany: *Kreiselpumpen, Berechnung und Konstruktion*, 3. Auflage)

ACKNOWLEDGEMENTS

We gratefully acknowledge the Elwetritsch-Cluster in Kaiserslautern, where all numerical investigations have been performed
We gratefully acknowledge the cooperation with SERO Pump Systems, who provided the pump and many other information.